Journal of Chromatography A, 1218 (2011) 2626–2634

Contents lists available at ScienceDirect

Journal of Chromatography A

journal homepage: www.elsevier.com/locate/chroma

Short communication

Rapid sequential separation of essential oil compounds using continuous heart-cut multi-dimensional gas chromatography–mass spectrometry

Seung-Ok Yang[a], Yujin Kim[a], Hee-su Kim[a], Sun-Hee Hyun[a], So-Hyun Kim[a], Hyung-Kyoon Choi[a,*], Philip J. Marriott[a,b,**]

[a] College of Pharmacy (WCU Laboratory), Chung-Ang University, Seoul 156-756, South Korea
[b] Centre for Green Chemistry, School of Chemistry, Monash University, Wellington Road, Clayton VIC 3800, Australia

ARTICLE INFO

Article history:
Received 15 October 2010
Received in revised form 28 January 2011
Accepted 23 February 2011
Available online 2 March 2011

Keywords:
Essential oil
Cryogenic modulation
Modulation period (P_M)
Multidimensional gas
Chromatography–mass spectrometry
Cryotrapping
Continuous heart-cutting

ABSTRACT

A method for separation and identification of peaks in essential oil samples based on rapid repetitive heart-cutting using multidimensional gas chromatography (MDGC)–mass spectrometry (MS) coupled with a cryotrapping interface is described. Lavender essential oil is analyzed by employing repetitive heart-cut intervals of 1.00 and 1.50 min, achieved in a parallel MDGC–MS/GC-FID experiment. The number of peaks that were detected in 1D GC operation above a given response threshold more than tripled when MDGC–MS employing the cryotrapping module method was used. In addition, MDGC–MS enabled detection of peaks that were not individually evident in 1D GC–MS, owing to effective deconvolution in time of previously overlapped peaks in 1D GC. Thus separation using the cryomodulation approach, without recourse to using deconvolution software, was possible. Peaks widths decreased by about 5–7-fold with the described method, peak capacity increased from about 9 per min to 60 per min, and greater sensitivity results. Repeatability of retention times for replicate analyses in the multidimensional mode was better than 0.02% RSD. The present study suggests that the described heart-cutting technique using MDGC–MS can be used for general improvement in separation and identification of volatile compounds.

1. Introduction

Gas chromatographic (GC) analysis with mass spectrometry (MS) is a well-established and reliable analysis method [1,2]. However innovation continues to introduce new capabilities in both GC and MS, and these evolving developments push technical demands in this area. Fast GC necessitates fast scanning MS systems, and both faster scanning quadrupole and time-of-flight MS have been introduced to cater for this need [3]. Improved detection limits based on selected ion monitoring, and use of triple quadrupole and $(MS)^n$ methods employing the specificity of precursor/product ion relationships, in the presence of complex matrix interferences [4–7] can overcome the lack of chromatographic separation power though such approaches lose the ability to provide library confirmation of a full scan MS method.

In GC, the problem of compound identity can only be addressed by improved separation of components, and a productive strategy is to employ a multidimensional GC (MDGC) separation approach [8]. Whilst MDGC has also had a long history [9] a number of emerging methods have proved their worth in providing improved separation power. Thus comprehensive two-dimensional GC (GC × GC) gives a total peak separation capacity (^Tn) that has been quoted as the product of the capacities of the two columns defining the method (^1n and ^2n) [10] (i.e. $^1n = 500$, $^2n = 20$, so $^Tn = 10{,}000$). The ^{2}D column has limited capacity, so for an especially complex region of a chromatogram the classical approach of MDGC still should be the most appropriate, since a small region of the ^{1}D column elution can be transferred to a higher peak capacity ^{2}D column that exceeds the ability of GC × GC to resolve that target zone [11].

Successful implementation of the GC × GC method has been largely based on cryogenic trapping methods, with moving modulators, and single and dual jet systems mostly employed [12–14]. MDGC can effectively use this same technology for zone enrichment at the head of a second column, and translating the experience with GC × GC cryogenic methods suggests that new approaches to ultra fast methods for the cryotrapping and subsequent re-mobilization process should be applicable to MDGC.

The MDGC method isolates a small zone of ^{1}D column effluent, then introduces it into a ^{2}D column. The faster the separation process demanded on the ^{2}D column, the narrower the zone (i.e. fewer peaks) sampled from the ^{1}D column should be, since this maximizes statistical peak separation on the ^{2}D column. Consequently a nar-

* Corresponding author. Tel.: +82 2 820 5605.
** Corresponding author at: Centre for Green Chemistry, School of Chemistry, Monash University, Wellington Road, Clayton VIC. 3800, Australia. Tel.: +61 3 99059630.
E-mail addresses: hykychoi@cau.ac.kr (H.-K. Choi), Philip.Marriott@monash.edu (P.J. Marriott).

0021-9673/$ – see front matter © 2011 Elsevier B.V. All rights reserved.
doi:10.1016/j.chroma.2011.02.060

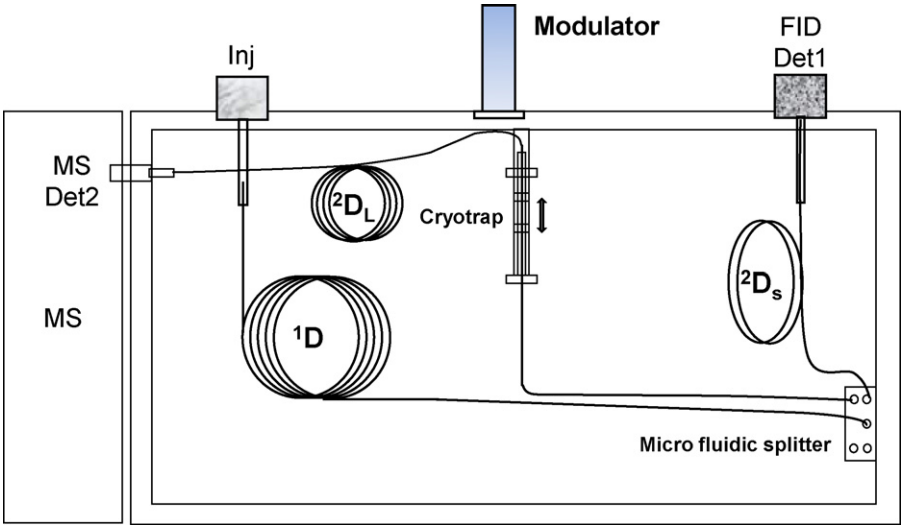

Fig. 1. Schematic diagram of the experimental MDGC set-up.

row bore column is suggested [15,16]. Cryotrapping methods are ideally suited to this requirement.

A previous method outlined by one of us described selection of a limited number of zones from a ^{1}D column using a mechanical valve, directing it into a cryotrap, then moving the cryotrap longitudinally along the column (towards the incoming carrier flow). This launched the cryotrapped components rapidly into the ^{2}D column, of dimensions about 5–10 m length and 0.1 mm ID [13,17–19]. It was shown that about 40 or more components could be separated in less than 1 min. The sampled ^{1}D column effluent can be as narrow as necessary, and the ^{2}D column can be as long as needed to achieve, or maximize, separation [20]. A method using a Deans switch was proposed for fragrance products with 5 heart-cuts taken in regions of suspected allergens [21]. The above methods were demonstrated for an FID detector, but not for a MS detector.

More recently, Striebich et al. [22] reported use of a system not unlike the one used in the previous work, incorporating a time-of-flight MS for aviation fuel analysis. A trapping interval of 15 s was employed, that was claimed to be about the duration of one peak width. A switchable GC × GC/MDGC operation in a single system was also reported; a region of a chromatogram that required greater separation performance than provided by a short ^{2}D column in GC × GC, could be selected for transfer to a longer – but still relatively fast – ^{2}D column [23].

This study applies MDGC to a lavender oil sample with parallel FID and MS detection, in a continual cryogenic sampling process from the ^{1}D column. All compounds are transferred to the ^{2}D column, no decision is made regarding target zone for transfer, and no microfluidic switching valve is required.

2. Experimental

2.1. GC/MS system

An Agilent Technologies 7890A model GC (Agilent Technologies, Seoul, Korea) equipped with one flame ionization detector, a 5975C MSD detector, 7683B series auto sampler, one injection module, and Chemstation software was used. The GC was retrofitted with an Everest model longitudinally modulated cryogenic system (Chromatography Concepts, Doncaster, Australia), and splitter (3-way splitter: Part. No.: G3183-64010, Agilent). The GC was equipped with a split/splitless injector, operated at 250 °C; an injection volume of 1.0 μL was employed usually in split mode (1:10 split). The carrier gas was helium, and the column head pressure was 35.0 psi. The pressure at the midpoint (splitter) to the FID and MSD was the same, calculated to be 25 psi. The total flow supplied to the column was 1.0 mL min^{-1} throughout although different flows were initially tested to ensure elution on the ^2D_L column (see Section 2.2) within a reasonable time. GC temperature program rates of 3.0 and 5.0 °C/min were tested, with the former chosen for the remainder of the study, with an initial temperature of 60 °C (hold time 0 min) to a final temperature of 220 °C (hold time 5 min).

The flow to the FID and MSD channels was in an approximate ratio of 6:1 according to the relative column dimensions, thus a larger portion of the total sample is directed to the shorter ^{2}D column.

The FID was operated at 100 Hz, whilst the MS was operated at 23.79 Hz, over a mass acquisition range of 35–250 *m*/*z*, according to the maximum acquisition rate option.

The schematic diagram of this equipment is based on that reported in an earlier study [24], and is shown in Fig. 1. In contrast with that prior study, the present system incorporates two ^{2}D columns, with a longer column (^2D_L) located after the modulator and terminated at the MSD, and a shorter column (^2D_S) between the splitter and the FID in Fig. 1 orientation. The differences between the earlier report and this study are the use of the mass spectrometer system, a microfluidic splitter union rather than a mechanical switching valve, and continuous timed modulation. In a second operation, the two ^{2}D columns were swapped, so that the longer column passing through the modulator now terminated at the FID (refer to Fig. S-1 Supplementary Information) with modulation on the ^2D_L-FID channel.

2.2. Column information

The column set consisted of a ^{1}D fused silica capillary column of (5%-phenyl)-methylpolysiloxane (DB-5) phase (0.25 μm film thickness, d_f) with dimensions 30 m × 0.25 mm i.d., and two ^{2}D columns as follows: a DB-WAX phase (0.10 μm d_f) of dimensions 1.0 m × 0.10 mm i.d. connected to the FID (^2D_S – short); a ^2D_L (long) separation column, of DB-WAX phase (0.10 μm d_f) of dimensions 7.0 m × 0.10 mm i.d. (6.50 m effective length). The ^2D_L column was fed through the cryotrap, then connected to the MSD. All columns were from Agilent Technologies.

2.3. Samples

As a reasonably complex application sample, lavender essential oil was used. The lavender essential oil was obtained from The Face

Shop Korea Co. Ltd. (Seoul, Korea). The lavender oil sample was prepared for analysis by diluting various volumes of lavender oil in hexane (99.9%; Burdick & Jackson, Muskegon, MI) to a total volume of 1000 μL. A 20% v/v solution was selected for most injections. Samples were then injected by split or splitless mode into the GC column, with split injection normally employed (usually 1:10 split ratio, but 20:1 was also used for a number of analyses).

A Fluka alkane standard mix (C8–C20; 40 mg/L in hexane; Labplus, Korea) was used for comparative cryotrapping studies.

A test sample comprising linalool, γ-terpinene, β-pinene, limonene and m-cymene (all obtained from TCI, Tokyo) was prepared at 0.26% v/v of each component in hexane, with camphor at 0.8% m/v.

2.4. Description of operation

Both single dimension analysis (1D) and target multidimensional analysis were conducted. For 1D GC/MS analysis the same dual column ensemble was used, but without implementation of the cryogenic fluid supply. The two orientations of the system shown in Fig. 1 were ^1D–^2D_S-FID and ^1D–^2D_L-MS, and are designated as such in figure legends and text.

For continuous multidimensional analysis, heart-cuts of 1.00 min or 1.50 min duration were conducted, commencing at 5.00 min. The split effluent from the ^1D column is directed to both the ^2D_S-FID and the ^2D_L-MS columns (split ratio approximately 6:1 in favour of the ^2D_S column). The modulator sequentially focuses the effluent into 1.00 or 1.50 min fractions, before launching the fractions into the ^2D_L column, simply by oscillating back and forth along the column at the appropriate timing interval. Effluent directed to the ^2D_S column does not undergo modulation, so approximates a continuous monitor FID channel for the chromatographic result at the end of the ^1D column.

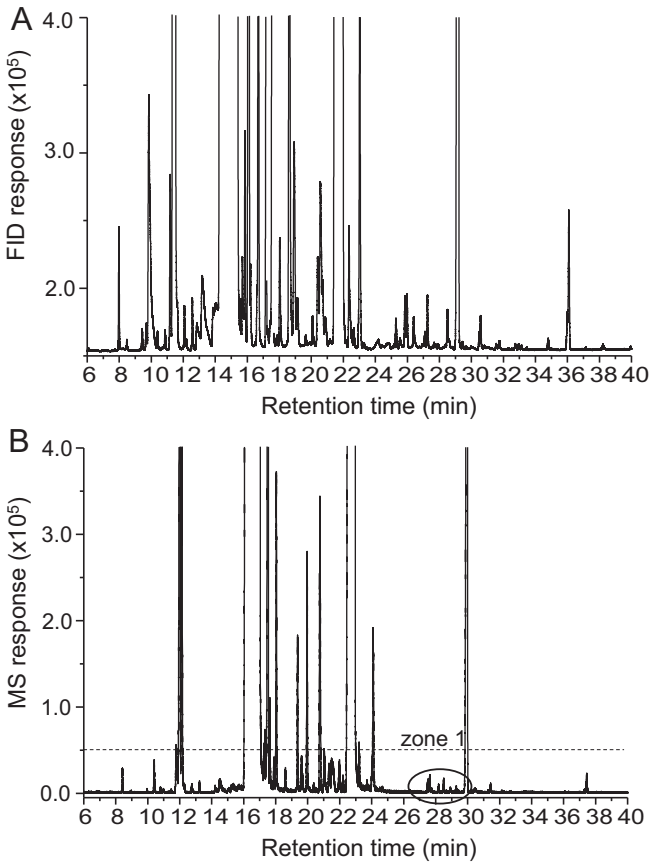

Fig. 2. Gas chromatogram of lavender essential oil analyzed by (A) ^1D GC-FID through ^2D_s column, (B) ^1D GC/MS through ^2D_Lcolumn according to Fig. 1 arrangement.

3. Results and discussion

Lavender oil was first analyzed using the GC/MS in order to provide a screening analysis of the minor components of lavender at a temperature programming rate of 3 °C/min. Similar to other essential oils, many compounds are contained in the lavender oil sample as shown in Fig. 2 result. In this and many other chromatograms presented here, the response scale is expanded to enable low response peaks to be more easily recognized. Fig. 2(A) and (B) is the FID and MS responses respectively, on which relative responses can be ascertained and compared with later data.

3.1. Standard compound analysis

Fig. 3 is the GC result for the six standard compounds – β-pinene, limonene, m-cymene, γ-terpinene, linalool, and camphor – with CO_2 cryotrapping in the ^2D_L channel. Fig. 3(A) is the ^1D–^2D_S-FID chromatogram approximating the monitor result at the end of the ^1D column. The peak shown in the boxed region is β-pinene, which has a time of 9.00 min. β-Pinene is separated into two peaks at the end of the ^2D_L column (Fig. 3(AI)). Since the cryodevice performs a heart-cut at exactly 9.00 min, and the peak elution time at the end of the ^1D column is also 9.00 min, there will be two distinct components generated for β-pinene (1(a) and 1(b)). Modulation occurs every 1.00 min, so these two peaks should appear at almost 1.00 min apart. t_R values are 9.527 min and 10.508 min respectively, with Δt_R = 0.981 min; the later peak therefore elutes with slightly faster retention due to the higher oven temperature of the ^2D_L column at this time.

The ^2t_R value for β-pinene is determined from the release time (9.00 min) to the total time of appearance of the peak on the MS (9.527 min). The release time is effectively the 'zero time' that the peak is introduced into the ^2D column. Thus ^2t_R (β-pinene) = 0.527 min. Estimation of the unretained peak time on the ^2D_L column is 17 s (note that most flow is to the ^2D_S FID channel), allowing retention factors to be calculated. Each component in Fig. 3(AI) has its own unique ^2t_R value, estimated to be limonene = 0.626 min, m-cymene = 0.774 min, γ-terpinene = 0.684 min, linalool = 1.779 min, and camphor = 1.400 min. Retention factors are 0.82, 1.16, 1.67, 1.36, 5.13 and 3.83 respectively. For the last two solutes, since the modulation time is known from the FID appearance of the peak, this determines the modulation event time, which is subtracted from the MS retention time. Limonene and m-cymene swap position on the two column phases, corresponding to the greater polarity of the m-cymene molecule arising from its aromatic property. Both limonene and m-cymene trap together in one collection event, so m-cymene will have a greater partition coefficient on the ^2D phase at the operating temperature.

In Fig. 3(BI) heart-cut timing at 1.50 min intervals is presented, with (B) the respective ^1D–^2D_S-FID channel. Now the modulation process does not divide the β-pinene peak so it gives a single peak. Fig. 3(A) and (B) results apparently arise from slightly different flow rates and operational conditions, with Fig. 3(A) suggested to be at a higher gas linear velocity, which results in slightly later retentions in Fig. 3(B). For Fig. 3(A) a higher split ratio of 20:1 was employed, but with the same nominal column volume flow rate and velocity. It appears that exactly the same linear flow velocity was not achieved, giving slightly faster retentions in Fig. 3(A). Nonetheless, the same interpretation as above can be inferred, with again the ^2t_R values readily derived; these are β-pinene = 0.519 min, limonene = 0.582 min, m-

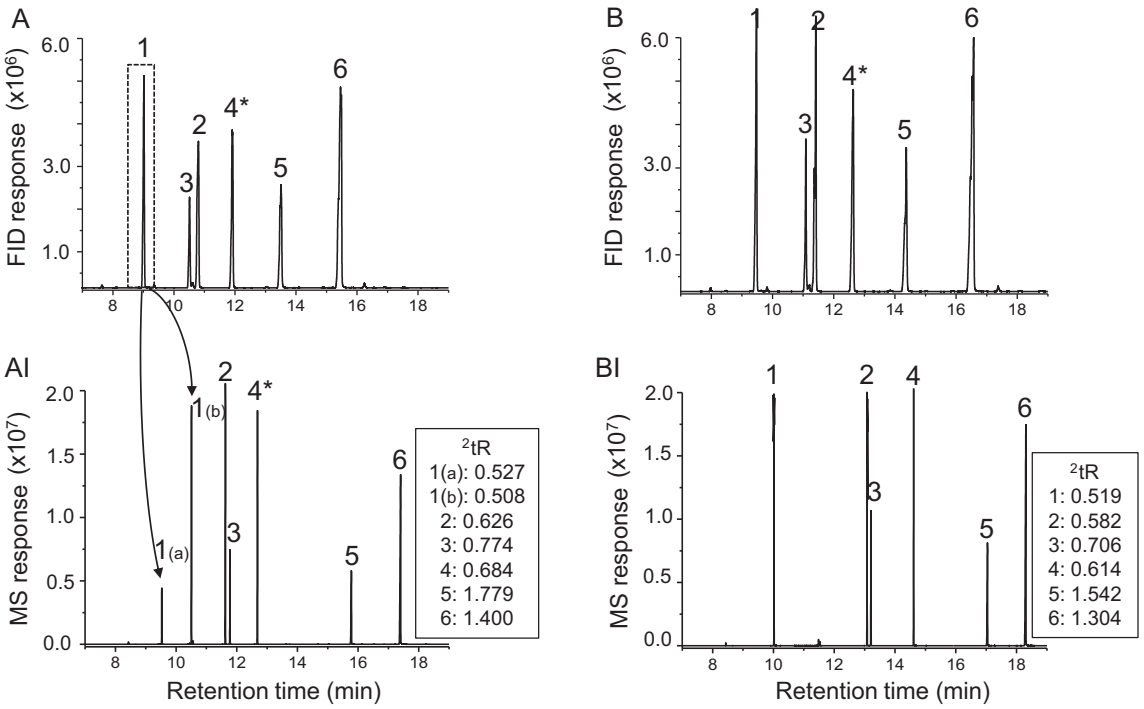

Fig. 3. Gas chromatogram of the six standard compounds mixture analyzed by MDGC–MS according to Fig. 1. (A) and (B) ^{1}D–$^{2}D_{s}$-FID data; (AI) ^{1}D–$^{2}D_{L}$-MS (1.0 min); (BI) ^{1}D–$^{2}D_{L}$-MS (1.5 min). 1: β-pinene; 2: limonene; 3: m-cymene; 4: γ-terpinene; 5: linalool; 6: camphor.

cymene = 0.706 min, γ-terpinene = 0.614 min, linalool = 1.542 min, and camphor = 1.304 min. If release into the ^{2}D column occurs at a higher oven temperature condition for a given component, then $^{2}t_R$ will be marginally lower, as seen for the second of the β-pinene peaks in Fig. 3(AI). Modulation periods (P_M) of 1.00 and 1.50 min, commencing at 5.00 min, should mean that modulation is synchronized every 3.0 min, starting from the commencement time of 5.0 min, then at 8.0, 11.0, 14.0, 17.0 min etc. thereafter. If a particular peak is released to the ^{2}D column when the modulations are synchronized, then retention times on ^{2}D should be the same, provided flow and temperature conditions are the same. This is confirmed for lavender data later.

Peak widths at half peak heights for compounds at the FID are much broader than for the MS detector; e.g. for peak 4 in Fig. 3(A) and (AI), values are 3.00 and 0.40 s respectively; MS $w_{½} \sim 7\times$ narrower. Peak width on the FID arises from broadening processes on the long ^{1}D column plus the additional short $^{2}D_S$ column. However, peak width at the MS will essentially only arise from dispersion/diffusion on the relatively shorter narrow bore $^{2}D_L$ column, since the sampled ^{1}D zone is compressed into a sharp band in the cryomodulator, then instantaneously released. An approximate measure of efficiency (theoretical plates) can be calculated for the above result (although should not normally be applied in a temperature programmed case); β-pinene $^{2}t_R$ = 0.527 min = 31.6 s; $w_{½}$ = 0.40 s so N = 34,600 or 5300/m. This is less than predicted for a 0.1 mm ID column at optimum conditions, but the source of this discrepancy is not clear. Gas average flow velocity appears above optimum, estimated at about 40 cm/s.

Similar data for the standard set of samples are presented for the case of swapping the detectors, according to Fig. S-2 (Supplementary Information).

3.2. Lavender sample analysis

Fig. 4 shows the GC result applied to the more complex lavender oil, with both 1.00 min and 1.50 min heart-cutting using the cryotrap. Fig. 4(A) is the FID result (no cryotrapping), whilst Fig. 4(BI) and (BII) is the results for 1.00 and 1.50 min cryomodulation. The circled region in Fig. 4(BI) can be compared with the same region in Fig. 2(B) (both are for MS detection, same volume injected), however signal enhancement due to cryogenic zone compression occurs in Fig. 4(BI), and resolution is much better. Fig. 4(BI) shows that the circled minor peaks have a response of about 100,000 compared to that in Fig. 2(B) of about <20,000. If an arbitrary signal response of 5×10^4 is taken as an assumed threshold for adequate detection, there are about 11 peaks greater than this threshold value in Fig. 2(B), whilst about 48 peaks are above this threshold in Fig. 4(BI). Some of these peaks could be due to 'split components' that might be counted twice (in 1.50 min modulation, there will be fewer of these split peaks), but this cannot account for the many more peaks above threshold that arise from the modulation experiment; they are due to the narrower peaks and signal magnitude enhancement.

The effect that the ^{2}D column has on peak identification in GC/MS operation can be gleaned from data in Tables 1 and 2. Table 1, without cryotrapping (i.e. in 1D mode) has the least number of tentatively identified components, at >70% match quality (only 11 components). With cryotrapping, Table 2 (1.00 and 1.50 min P_M) gives 28 and 23 peaks respectively at the same minimum match

Table 1
Chromatographic data of peaks of lavender oil (in Fig. 2(B)) analyzed using one dimensional gas chromatography (over 70% matching quality using ADAMS library).

Peak no.	t_R	Compounds	Match (%)
1	8.414	α-Pinene	83
2	11.765	6-Methyl-5-hepten-2-ol	94
3	11.998	Limonene	97
4	12.134	1,8-Cineole	90
5	17.016	Linalool	86
6	18.038	Camphor	94
7	19.372	Isoborneol	83
8	21.027	γ-Terpineol	74
9	22.957	Linalool acetate	91
10	28.504	Geraniol	72
11	29.963	Iso-caryophyllene	94

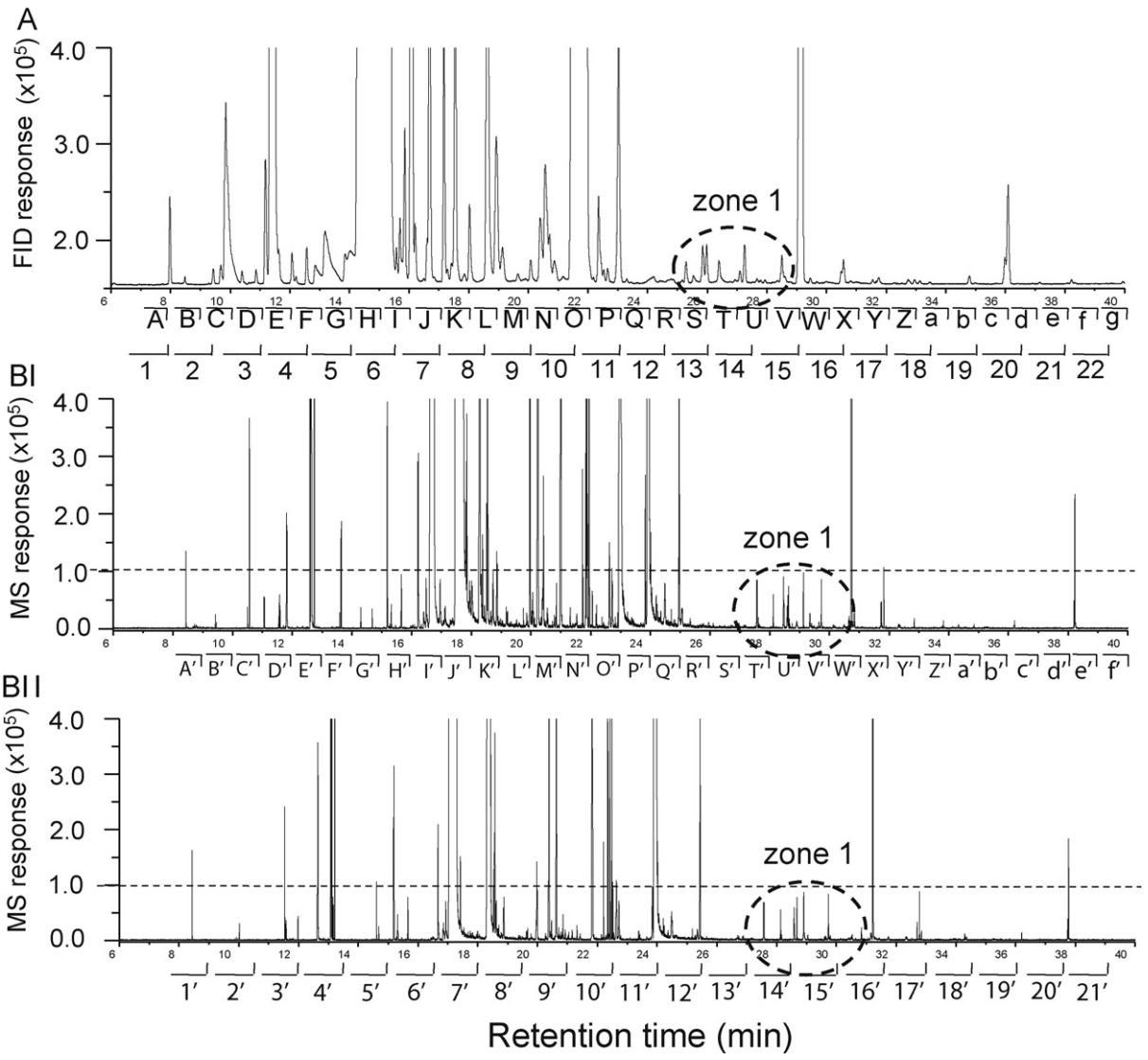

Fig. 4. Gas chromatogram of lavender essential oil analyzed by 1D GC and MDGC according to Fig. 1. (A) ^{1}D–^{2}D$_{s}$-FID; (B) MDGC showing ^{1}D–^{2}D$_{L}$-MS with cryotrapping (BI: 1.00 min modulation), (BII: 1.50 min modulation). Zones A–g indicate 1.00 min modulation; zones 1–22 indicate 1.50 min modulation. The corresponding apostrophe designations indicate these same zones collected and released to the MS.

statistic. The greater peak response should be largely responsible for this result, and by choosing a response threshold of 50,000, about 11 peaks were above this value (Fig. 2(B)), whereas about 48 peaks had response above 50,000 in Fig. 4(BI), and about 32 in Fig. 4(BII). A usual injection-to-injection volume uncertainty in the latter case seems to explain the fewer peaks above 50,000, this was still well in excess of the 1D GC case.

Zones that indicate both 1.00 min (A–g) and 1.50 min (1–22) sampled modulation regions are shown below the time axis in Fig. 4(A), and the resulting regions offset by 1.00 or 1.50 min respectively are shown as A′–f′, and 1′–21′ in Fig. 4(BI) and (BII). Fig. S-3 (Supplementary Information) illustrates the analogous GC/MS and GC-FID responses for the swapped detectors, where the FID now reports the cryomodulated ^{2}D$_{L}$ data. It is easier to note the small peaks that can be seen on the FID compared with the number that are shown with the MS detector, in contrast with the non-modulated ^{1}D–^{2}D$_{S}$-FID result. The swapping of detectors (S.I.) allows the same detector to be contrasted for the two different length ^{2}D columns, and the performance of the modulated response on the FID which has less noise.

3.3. Expanded plots of modulated regions

Fig. 5(A–BII) is expansion region of Fig. 4(A–BII) heart-cuts taken over 12.0–14.0 min, to allow more detail to be displayed. Superimposed in Fig. 5 are dashed lines that show 1.00 min modulation, and dotted lines that show 1.50 min timed modulation. Fig. 5(BI) and (BII) is offset by the 1.00 and 1.50 min durations that the modulator is held in position. Thus sampled regions F and G in Fig. 5(A) are then released to ^{2}D$_{L}$ and should correspond to regions F′ and G′ in Fig. 5(BI), and zone 5 in Fig. 5(A) should correspond to 5′ in Fig. 5(BII). Since there is no guarantee that a compound will elute from ^{2}D$_{L}$ within one P_{M}, zone H′ is also shown in Fig. 5(BI). It seems reasonable to assign the asterisked peak in Fig. 5(A) with those in both Fig. 5(BI) and (BII). This can be justified by considering the retention of this peak in (BI) and (BII); it occurs at ∼ 0.6 min after modulation in (BI), and at about 0.6 min after modulation in (BII). The large broad peak (#) in Fig. 5(A) must elute in zone H′ – i.e. it elutes later than 1.0 min on ^{2}D$_{L}$ since no large peak appears in zone G′. Modulations are synchronized at 14.00 min in Fig. 5(BI) and (BII), so the large # peak that is trapped in region 5 under 1.5 min mod-

Table 2
Chromatographic data of peaks of lavender oil (Fig. 4 (BI) and (BII)) analyzed using multidimensional gas chromatography with 1.0 min and 1.5 min heart-cut interval (over 70% matching quality using ADAMS library).

Compounds	1.0 min			1.5 min		
	t_R (min)	^2t_R (min)[a]	Match (%)	t_R (min)	^2t_R (min)	Match (%)
α-Pinene	8.432	0.432	94	8.433	0.433	96
6-Methyl-5-hepten-2-one	11.058	1.058	90	11.979	0.979	72
α-Phellandrene	11.558	0.558	78	11.558	0.558	90
para-Mentha-2,4(8)-diene	11.583	0.583	72	11.582	0.582	80
6-Methyl-5-hepten-2-ol	11.815	1.815	95	12.643	1.643	95
Limonene	12.595	0.595	97	13.081	0.581	97
1,8-Cineole	12.624	0.624	90	13.110	0.61	90
(e)-β-Ocimene				13.156		90
ortho-Cymene	12.734	0.734	91	13.215	0.715	87
γ-Terpinene	13.638	0.638	94	14.607	0.607	94
Terpinolene[b]	14.683	0.683	91	14.683	0.683	86
cis-Linalool oxide furanoid	15.316	0.316/1.316[c]	78	16.669	1.169	83
Linalool	16.680	0.680/1.680[c]	87	18.400	1.400	91
cis-Pinan-2-ol	18.381		74			
Hexyl isobutyrate	19.747		72			
Isoborneol	19.967		94			
trans-β-Terpineol	20.064		72			
Terpinen-4-ol	20.417	1.417	87	19.980	1.480	87
trans-Linalool oxide pyranoid				20.926		78
α-Terpineol				21.823		86
Camphene	22.909		81			
Iso-dihydro carveol acetate	24.972	0.972	89	25.440	0.94	76
Lavandulyl acetate[d]	28.117	1.117	90	28.681	1.181	83
α-Copaene	28.623		90			
Lavandulyl acetate[d]	29.134	1.134	72			
Valencene	29.734		93			
Iso-caryophyllene	30.743	0.743	93	31.225	0.725	93
(e)-β-Farnesene	31.738		74			
α-Humulene	31.819	0.819	95	32.778	0.778	90
γ-Amorphene				32.846		80
Caryophyllene oxide	38.232	1.232	76	37.775	1.275	90

[a] ^2t_R data are presented only for compounds that are found in both 1.00 and 1.50 min modulation data apart from lavandulyl acetate.
[b] The 1.00 min experiment matched α-terpinene; the 1.50 min experiment matched terpinolene, but their similarity of spectra and of retention suggests they are the same component.
[c] Two values are often possible, especially for strongly retained components. The value for 1.50 min operation helps to decide the correct option.
[d] These two peaks are due to splitting of the lavandulyl acetate component.

ulation, is also released into the ^2D_L column at 14.00 min – just as in Fig. 5(BI). Hence the large peak appears at the same retention of about 15.2 min in both cases, and this suggests a ^2t_R of ~1.2 min.

The asterisked peak in Fig. 5(A) has a width at half peak height of 4.00 s, and in Fig. 5(BII) is about 0.75 s, confirming the sharpening of the peak after cryogenic modulation. Figs. S-4 and S-5 display the analogous MDGC-FID cryotrapping experimental results for comparison.

Similarly Fig. 6 describes results for the interval 19.0–21.5 min. Fig. 6(A) has a reasonably complex region in the N zone. Perhaps 5 peaks can be suspected here, with only one (the first) apparently fully resolved. Zone M′ in Fig. 6(BI) has two very large peaks at 20.2 and 21.0 min. These are not seen in Fig. 6(A), so must arise from the preceding zones K and L. This can be seen in Fig. 4(A), where two large (and closely eluting) peaks can be seen in region L. The peak at 21.0 min therefore has a ^2t_R of >1.0 min. Zone N′ has about 7 peaks (5 resolved peaks, and 2 almost resolved), all of which are much narrower and better resolved than those in zone N. The same group of peaks can be seen in Fig. 6(BII), arising from region 10 shown in Fig. 6(A), however they are at later retention times, arising from the delay before zone 10′ is released to the ^2D column. The contrast of this complex region in terms of resolution, and in response magnitude over that in Fig. 6(A), is striking. Peak capacity for 6(A) is about 9 peaks/min, whereas for 6(BI) it is about 60 peaks/min, demonstrating the improved separation power of the method.

For further reference, Fig. S-6 shows analogous results for the region 26.0–29.0 min, covering zones T–V (1.00 min P_M), and 14 and 15 (1.50 min P_M).

Repeatability data for triplicate analyses are shown in Table 3 for both 1.00 and 1.50 min P_M. Areas relate to the repeatability of injection volumes and retention repeatability relates to qualitative identification of peaks. Precision of t_R to within 0.001% is observed for 1.00 P_M (i.e. <0.1 s) indicating that the results are well preserved throughout the three runs. Region N′ for the 1.00 min and region 10′ for 1.50 min P_M are presented. Area repeatability is about 5% or less, as expected for injection volume repeatability.

Table 2 also reports estimated absolute retention times of most of the components on the ^2D_L column, following the procedure described for Fig. 3 (^2t_R = total retention time–modulator event time for introduction to the ^2D_L column). These assigned ^2t_R retention values are reported for components identified with library matches as common components across the two modulation experiments. In some cases where modulations are synchronized it will be difficult to decide if the retention should be incremented by 1.00 min, but in most cases only one option will be obvious; 1.00 and 1.50 modulation timing is synchronized at 8.00 min, so β-pinene will have the same ^2t_R under both modulation procedures (as seen in Table 2). Likewise α-phellandrene modulation occurs at 11.00 min for both modulation procedures and again has the same ^2t_R values. In many cases the ^2t_R retention of a component will be less under 1.50 min operation due to the higher elution temperature, for instance refer to the limonene results. Magnitude of retention can be supported by knowledge of the structure/polarity of the molecule, since polar molecules will be expected to have greater ^2t_R values on the polar ^2D_L phase. The case of linalool demonstrates that from the retention in the 1.00 min P_M case, the ^2t_R could be either 0.680, or 1.680 min. Since 1.50 min operation

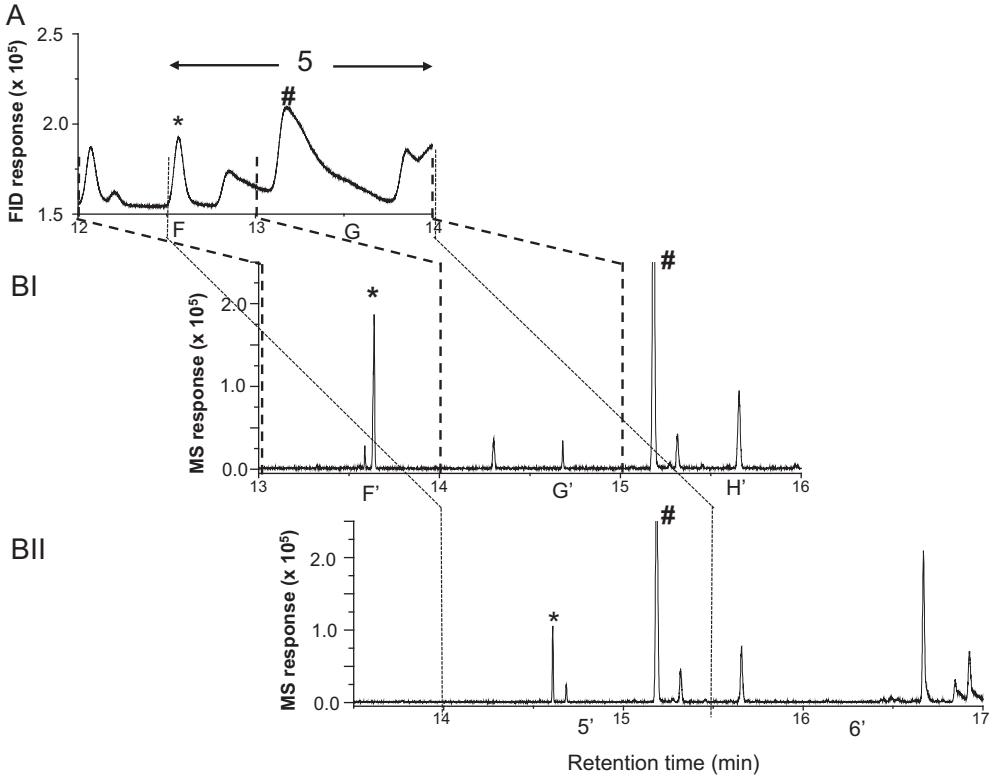

Fig. 5. Expansions of specific regions of Fig. 4. (A) FID zone F, G (1.00 min) and zone 5 (1.50 min); (BI) MDGC–MS zone F′ and G′ (1.00 min modulation); (BII) MDGC–MS zone 5′ (1.50 min modulation).

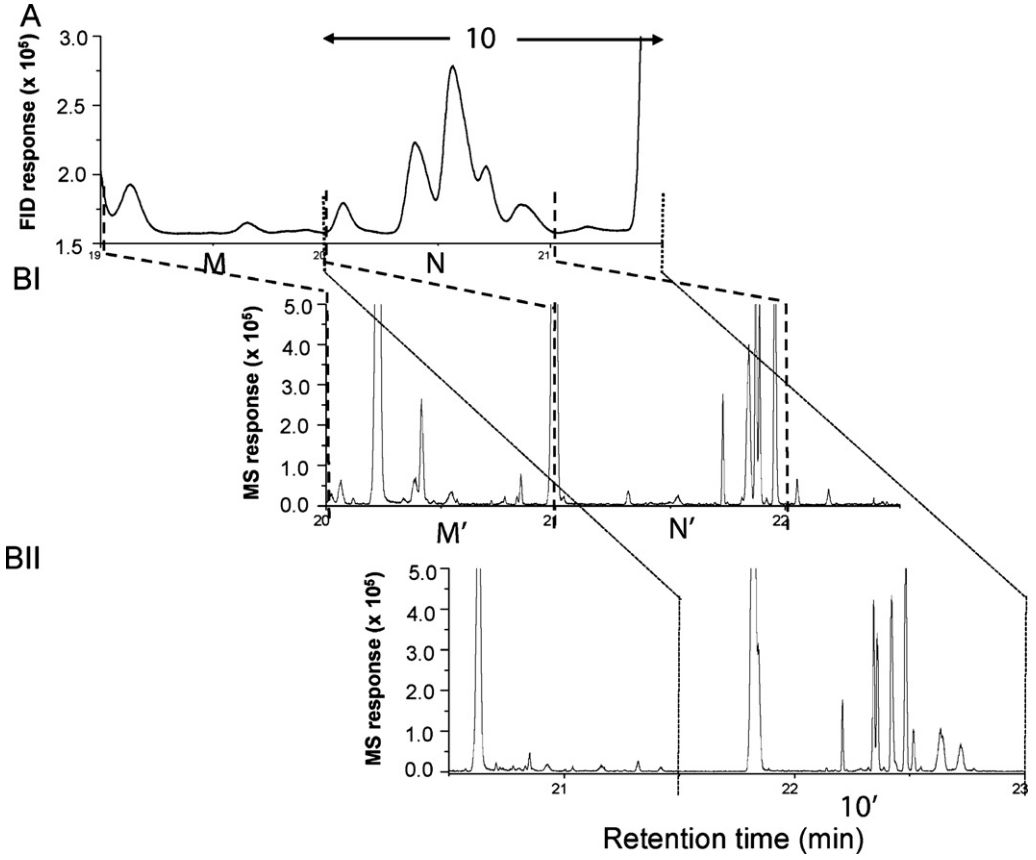

Fig. 6. Expansions of specific regions of Fig. 4. (A) FID zone M, N (1.00 min) and zone 10 (1.50 min); (BI) MDGC–MS zone M′ and N′ (1.00 min modulation); (BII) MDGC–MS zone 10′ (1.50 min modulation).

Table 3
Quantitative data for selected peak in heart-cut interval of 1.00 min N′ (Fig. 6(BI)) and heart-cut interval of 1.50 min 10′ (Fig. 6(BII)).

Peak No.	Replication 1		Replication 2		Replication 3		Area RSD %	t_R RSD %
	t_R	Area	t_R	Area	t_R	Area		
Heart-cut 1.0 min (N′)								
1	21.730	1,173,367	21.731	1,228,448	21.730	1,244,052	3.1	0.003
2	21.843	4,413,764	21.842	4,748,152	21.843	4,958,244	5.4	0.003
3	21.874	3,676,826	21.874	3,760,849	21.873	4,000,784	4.4	0.003
4	21.890	2,830,826	21.890	2,885,688	21.889	3,052,658	4.0	0.003
5	21.957	4,693,360	21.958	4,898,546	21.957	5,223,361	5.4	0.003
Heart-cut 1.5 min (10′)								
1	22.324	378,633	22.330	348,007	22.323	349,343	4.8	0.017
2	22.467	925,209	22.474	848,728	22.466	861,955	4.7	0.019
3	22.559	1,096,622	22.566	1,000,742	22.559	102,585	4.8	0.018
4	22.637	1,251,608	22.645	1,224,258	22.636	1,197,091	2.2	0.022

gives a ^2t_R value of 1.400 min, then ^2t_R must be 1.680 min when using 1.00 min operation. Most of the polar oxygenated compounds have ^2t_R values of about 1.0 min or more.

3.4. Alkane elution example

An example of cryotrapping C_9–C_{20} alkanes is shown in Fig S-7, (C-8 elutes before effective cooling of the modulator). Fig. S-7(A) is the non-modulated FID channel, showing the regular retention pattern of the homologues. The small concentration injected is noted from the low signal/noise (S/N) level of the FID response. In Fig. S-7(B) (^{1}D–^2D_L-MS) the cryotrap was operated until 32.0 min, at which time cryogen supply was halted. Narrower early peaks are again noted for Fig. S-7(B). The elution pattern of the alkanes will be expected to be affected by the modulation process. Retention time will now depend on the hold-up or delay period during which an alkane is held in the trapping region, and individual alkanes could have a variation in retention of up to about 1.00 min in the present case. (They will all have an added increment in retention compared to Fig S-7(A) due to the longer ^{2}D column.) Hence in Fig. S-7(B) retention times cannot be expected to represent the approximately linear increment in retention times expected in linearly temperature programmed analysis. Surprisingly, calibration plots of carbon number *vs.* retention time for Fig. S-7(A) and (B) have almost the same slope, and have R^2 values of 0.9987 and 0.999 respectively. Whilst this is surprisingly good, with no evidence of the modulation process affecting the quality of the calibration graph, it cannot be assumed that this means such a plot can be used reliably for derived properties for other solutes in the chromatogram, such as retention index calculations. This would have to be tested by separate experimentation.

The suitability of quadrupole MS (qMS) for the rate of elution of peaks into the MS, and to give unbiased scan data, was checked by plotting extracted ion data for scans on the up-slope and down-slope of an alkane peak. Data displayed good consistency of ion ratios, for the narrow peaks (peak width at half height $w_{½}$ ca. 0.4 s), and so bias was adjudicated to be minimal.

4. Conclusions

The present work extends prior studies on a method developed by one of us, conducted with peppermint oil using FID detection [20,24]. Confirmative assignment of peaks was not possible previously due to use of FID. The present study, employing qMS detection, demonstrates that satisfactory detection and library match quality could be attained with method objectives of enhanced resolution and improved response magnitude. Generally, the method should aim to ensure that elution of compounds is completed within the modulation cycle of the system. In the present case, both 1.00 and 1.50 min P_M were investigated, with polar compounds most retained on the ^{2}D polar column. A longer P_M risks collection of an excessive number of components during the sampling time, which then could cause overlapping of components when released to the second column. A shorter P_M gives less time to elute compounds on the ^{2}D column before the subsequent modulation event.

The present study permits a standard qMS to be used, and so should be applicable to many laboratories. This contrasts with techniques such as GC × GC which are best conducted with fast data acquisition e.g. time-of-flight MS systems, because of the very narrow peaks (e.g. $w_{½} \sim 0.1$ s) found in GC × GC, although GC × GC with high data acquisition rate qMS has also been described. The method is compatible with conventional data systems as opposed to the demands of GC × GC software processing. Thus a single peak is obtained for each compound (apart from those cases where a compound is split into 2 peaks; MS aids identification of each peak in this case).

Narrow peaks on the ^{2}D column, due to the cryogenic focusing process during the sampling stage, give $w_{½} \sim 0.3$–0.5 s, contributing to the improved separation power on the ^{2}D column and response increase.

A threshold response should correlate with detectability and also with identification of components, and it is shown that many more peaks are found above a given threshold when the described modulation method is employed. The present method should be applicable to routine investigation of volatile compounds in most GC experiments.

Acknowledgement

This research was supported by WCU (World Class University) program through the National Research Foundation of Korea funded by the Ministry of Education, Science and Technology (Grant Number: R33-10029).

Appendix A. Supplementary data

Supplementary data associated with this article can be found, in the online version, at doi:10.1016/j.chroma.2011.02.060.

References

[1] J.A.J. Trygg, J. Gullberg, A.I. Johansson, P. Jonsson, H. Antti, S.L. Marklund, T. Moritz, Anal. Chem. 77 (2005) 8086.
[2] M.M. Koek, B. Muilwijk, M.J. van der Werf, T. Hankemeier, Anal. Chem. 78 (2006) 1272.
[3] L. Mondello, P.Q. Tranchida, P. Dugo, G. Dugo, Mass Spectrom. Rev. 27 (2008) 101.
[4] T. Portolés, E. Pitarch, F.J. López, J.V. Sancho, F. Hernández, J. Mass Spectrom. 42 (2007) 1175.
[5] F. Hernández, T. Portolés, E. Pitarch, F.J. López, Anal. Chem. 79 (2007) 9494.
[6] F. Hernández, Ó.J. Pozo, J.V. Sancho, F.J. López, J.M. Marín, M. Ibáñez, TrAC Trends Anal. Chem. 24 (2005) 596.

[7] J.V. Sancho, Ó.J. Pozo, M. Ibáñez, F. Hernández, Anal. Bioanal. Chem. 386 (2006) 987.
[8] J.C. Giddings, Anal. Chem. 56 (1984) 1258A.
[9] L. Mondello, A.C. Lewis, K.D. Bartle, Multidimensional Chromatography, John Wiley & Sons Ltd., Chichester, 2002.
[10] J.C. Giddings, J. High Resolut. Chromatogr. 10 (1987) 319.
[11] R.E. Murphy, M.R. Schure, J.P. Foley, Anal. Chem. 70 (1998) 1585.
[12] M. Adahchour, J. Beens, R.J.J. Vreuls, U.A.T. Brinkman, Trend Anal. Chem. 25 (2006) 540.
[13] P.J. Marriott, R.M. Kinghorn, Anal. Chem. 69 (1997) 2582.
[14] R.M. Kinghorn, P.J. Marriott, P.A. Dawes, J. High Resolut. Chromatogr. 23 (2000) 245.
[15] D. Ryan, P. Morrison, P. Marriott, J. Chromatogr. A 1071 (2005) 47.
[16] M.M. Koek, B. Muilwijk, L.L.P. van Stee, T. Hankemeier, J. Chromatogr. A 1186 (2008) 420.
[17] P.J. Marriott, R.M. Kinghorn, J. Chromatogr. A 866 (2000) 203.
[18] P. Marriott, R. Kinghorn, TrAC Trends Anal. Chem. 18 (1999) 114.
[19] P.J. Marriott, R.C.Y. Ong, R.M. Kinghorn, P.D. Morrison, J. Chromatogr. A 892 (2000) 15.
[20] M. Dunn, R. Shellie, P. Morrison, P. Marriott, J. Chromatogr. A 1056 (2004) 163.
[21] M.S. Dunn, N. Vulic, R.A. Shellie, S. Whitehead, P. Morrison, P.J. Marriott, J. Chromatogr. A 1130 (2006) 122.
[22] R.C. Striebich, J. Contreras, L.M. Balster, Z. West, L.M. Shafer, S. Zabarnick, Energy Fuels 23 (2009) 5474.
[23] B. Maikhunthod, P.D. Morrison, D.M. Small, P.J. Marriott, J. Chromatogr. A 1217 (2010) 1522.
[24] P. Marriott, M. Dunn, R. Shellie, P. Morrison, Anal. Chem. 75 (2003) 5532.